Rapid Communications   Editors' Suggestion

Ferromagnetic ordering along the hard axis in the Kondo lattice YbIr$_3$Ge$_7$

Binod K. Rai,[1,*] Macy Stavinoha,[2,*] J. Banda,[3] D. Hafner,[3] Katherine A. Benavides,[4] D. A. Sokolov,[3] Julia Y. Chan,[4]
M. Brando,[3] C.-L. Huang,[1] and E. Morosan[1,2]

[1]*Department of Physics and Astronomy, Rice University, Houston, Texas 77005, USA*
[2]*Department of Chemistry, Rice University, Houston, Texas 77005, USA*
[3]*Max Planck Institute for Chemical Physics of Solids, Nöthnitzer Strasse 40, D-01187 Dresden, Germany*
[4]*Department of Chemistry and Biochemistry, University of Texas at Dallas, Richardson, Texas 75080, USA*

Ferromagnetic Kondo lattice compounds are far less common than their antiferromagnetic analogs. In this Rapid Communication, we report the discovery of a ferromagnetic Kondo lattice compound, YbIr$_3$Ge$_7$. As in almost all ferromagnetic Kondo lattice systems, YbIr$_3$Ge$_7$ shows magnetic order with moments aligned orthogonal to the crystal electric field (CEF) easy axis. YbIr$_3$Ge$_7$ is unique in that it is the only member of this class of compounds that crystallizes in a rhombohedral structure with a trigonal point symmetry of the magnetic site, and it lacks broken inversion symmetry at the local moment site. The ac magnetic susceptibility, magnetization, and specific heat measurements show that YbIr$_3$Ge$_7$ has a Kondo temperature $T_K \approx 14$ K and a Curie temperature $T_C = 2.4$ K. Ferromagnetic order occurs along the crystallographic [100] hard CEF axis despite the large CEF anisotropy of the ground-state Kramers doublet with a saturation moment along [001] almost four times larger than the one along [100]. This implies that a mechanism which considers the anisotropy in the exchange interaction to explain the hard-axis ordering is unlikely. On the other hand, the broad second-order phase transition at T_C favors a fluctuation-induced mechanism.

Various competing ground states in Kondo lattice (KL) systems, governed by the delicate balance between the Ruderman-Kittel-Kasuya-Yosida (RKKY) exchange interaction and on-site Kondo effect, have gained great interest for over three decades [1–3]. These two interactions usually result in antiferromagnetic (AFM) order with a dense KL metallic ground state. The balance between Kondo and RKKY interactions can be tuned by applying nonthermal parameters such as pressure, magnetic field, or chemical doping, resulting in non-Fermi-liquid behavior near a quantum critical point (QCP) where the AFM transition temperature is suppressed to absolute zero, or other quantum collective phenomena emerge including unconventional superconductivity [4–6].

Among known KLs, the number of compounds that shows AFM order greatly surpasses that of the ferromagnetically ordered compounds [7–9]. Thus, in stark contrast to the AFM counterpart, in-depth theoretical work to describe ferromagnetic (FM) KL compounds is largely missing [10,11]. Recently, Ahamed *et al.* [8] suggested that broken inversion symmetry at the local moment site could promote FM order in KLs. While this scenario is possible for most of the Ce- and Yb-based FM KL compounds, including CeTiGe$_3$ [12], YbNiSn [13], YbPtGe [14], YbRhSb [15], YbPdSi [16], and the most heavily studied FM KLs CeAgSb$_2$ [17–21], CeRuPO [22–24], and YbNi$_4$P$_2$ [25], it does not apply to systems *with* inversion symmetry such as Yb(Rh$_{0.73}$Co$_{0.27}$)$_2$Si$_2$ [26,27] and YbCu$_2$Si$_2$ [28,29]. Moreover, it has been theoretically and experimentally found that the FM phase is inherently unstable,

either towards a first-order phase transition [30] or towards inhomogeneous magnetic phases [31]. Thus, the FM QCP either does not exist or is masked by other phases. Only in the case of YbNi$_4$P$_2$, FM order occurs via a second-order phase transition upon chemical substitution in YbNi$_4$(P$_{1-x}$As$_x$)$_2$ [32]. The presence of a FM QCP in this system has been attributed to its quasi-one-dimensional (1D) structure [25,32]. Thus, in order to develop the theory surrounding FM KL systems in general, and experimentally realize new FM QCPs in particular, new FM KL compounds are called for.

In compounds with strong crystal electric field (CEF) effects, the CEF-induced anisotropy determines the direction of easy and hard magnetization axes in the paramagnetic (PM) state. Interestingly, in all of the FM KL compounds mentioned above, with the exception of CeTiGe$_3$ and YbCu$_2$Si$_2$, this CEF anisotropy competes with the RKKY interaction and results in magnetic ordering along the axis *orthogonal* to the CEF easy axis [17,22,25,27,32,33]. Even more astonishing is the fact that the FM hard-axis ordering appears to be a general trait of FM KL systems, as of yet unexplained [9].

In this Rapid Communication, we report the discovery of a FM KL compound YbIr$_3$Ge$_7$ with $T_C = 2.4$ K. In line with the above empirical observation, spontaneous magnetization occurs along the hard CEF axis. However, YbIr$_3$Ge$_7$ is unique among FM KLs because it is the only such compound crystallizing in a rhombohedral lattice, and it does not show broken inversion symmetry at the local moment site. Recently, we discovered a series of Ce- and Yb-based compounds in this 1-3-7 structural family, including YbRh$_3$Si$_7$ [34], CeIr$_3$Ge$_7$ [35,36], and YbIr$_3$Si$_7$ [37]. Among these compounds, YbRh$_3$Si$_7$ and YbIr$_3$Si$_7$ show Kondo screening with the former proposed

---

*These authors contributed equally to this work.

to order antiferromagnetically below 7.5 K based on neutron scattering, and the latter showing long-range magnetic order below 4 K. In contrast, $CeIr_3Ge_7$ shows AFM order along the easy CEF axis at a remarkably low temperature $T_N = 0.63$ K, in the absence of Kondo screening or frustration. Although chemically and structurally similar, the balance between CEF effects, Kondo screening, and RKKY interactions in these systems differ drastically. Thus, this family of compounds presents an opportunity to study the delicate competition among these interactions and the resulting ground states.

Single crystals of $YbIr_3Ge_7$ were grown using Ge self-flux, as described in earlier publications [38,39] and the Supplemental Material [40]. The purity and crystal structure were identified by single crystal and powder x-ray diffraction analysis (Tables S1 and S2, Figs. S1 and S2 in the Supplemental Material). $YbIr_3Ge_7$ crystallizes in the $ScRh_3Si_7$ structure type [41,42] with lattice parameters $a = 7.8062(10)$ Å and $c = 20.621(5)$ Å. The stoichiometry determined by free variable refinement of the occupancies is $YbIr_3Ge_{7-\delta}$, where $\delta = 0.3$. The crystals were oriented along the [100] and [001] axes in the equivalent hexagonal unit cell setting using a backscattering Laue camera. Powder x-ray diffraction data were collected at room temperature using a Bruker D8 diffractometer with Cu $K\alpha$ radiation, with additional single crystal x-ray diffraction performed at room temperature using a Bruker D8 Quest Kappa single crystal x-ray diffractometer equipped with an IμS microfocus source, a HELIOS optics monochromator, and a complementary metal-oxide semiconductor (CMOS) detector. The anisotropic dc magnetic susceptibility M/H and magnetization data were measured using a Quantum Design (QD) magnetic property measurement system (MPMS) with an applied magnetic field up to 7 T. The ac susceptibility was measured with a QD MPMS with a modulation field amplitude $\mu_0 H_{ac} = 1$ mT at a frequency of 113.7 Hz. The ac susceptibility measurements at 20 mK were performed using an Oxford Instruments dilution refrigerator. Specific heat and electrical transport measurements were performed in a QD physical property measurement system.

In $YbIr_3Ge_7$, the Yb atom occupies a trigonal point symmetry ($\bar{3}$), and the $J = 7/2$ energy levels are split by the CEF in four Kramers doublets. While the CEF energy levels for the Ce isostructural compound were determined from magnetic susceptibility measurements and calculations [35,36], the larger angular momentum of the Yb leads to a corresponding Hamiltonian with six parameters in $YbIr_3Ge_7$, which cannot be fully solved with the data at hand. However, large CEF anisotropy in $YbIr_3Ge_7$ is evidenced by the linear high-temperature inverse susceptibility $H/(M - M_0)$ shown in Fig. 1(a), measured for field $H \parallel [001]$ (blue symbols) and $H \parallel [100]$ (red symbols). The Curie-Weiss fit (solid line) of the average inverse susceptibility (purple) between 400 and 600 K yields the experimental effective moment $\mu_{eff} = 4.42\mu_B$/Yb, close to the calculated value $4.54\mu_B$/Yb for Yb^{3+}. The paramagnetic Weiss temperatures along [100] and [001] are both negative, $\theta_W^{[100]} = -400$ K and $\theta_W^{[001]} = -70$ K, and yield a first CEF parameter $B_2^0 = -1.6$ meV [43], which is a measure of the strength of the CEF anisotropy. Deviations from linearity below 300 K indicate that CEF splitting exceeds this temperature range, similar to the large splitting observed in the Ce analog [35,36].
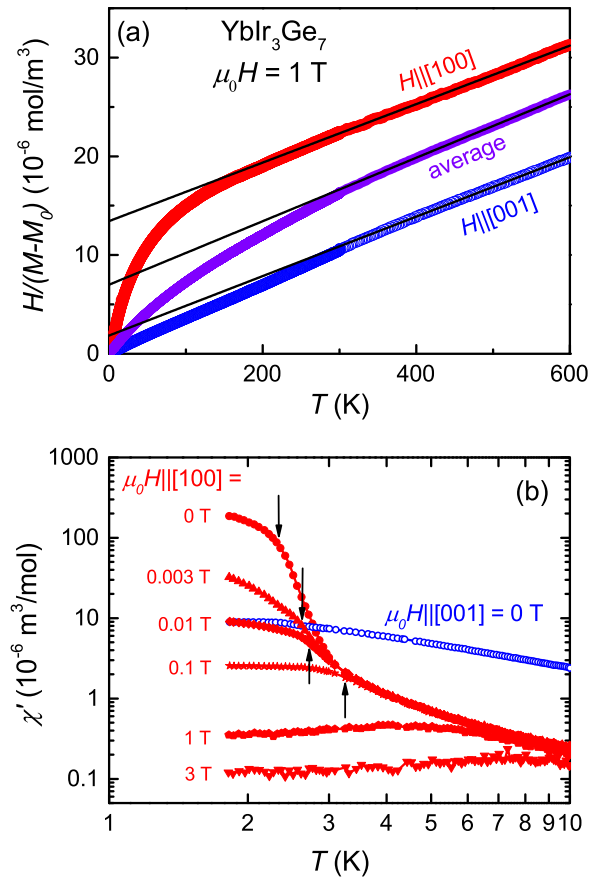

FIG. 1. (a) Inverse magnetic susceptibility $H/(M - M_0)$ vs T with the polycrystalline average $M_{avg} = (M_{001} + 2M_{100})/3$ (purple line) and Curie-Weiss fits between $T = 400$ and 600 K (solid black lines). (b) Temperature-dependent ac magnetic susceptibility χ' with H_{ac} along [001] (blue open symbols) and along [100] (red solid symbols) with different applied static fields H applied also along [100].

Further insight into the low-temperature magnetic properties of $YbIr_3Ge_7$ comes from the magnetic ac susceptibility shown in Fig. 1(b). The ac susceptibility measurements reveal spontaneous magnetization below $T_C = 2.4$ K for $H \parallel [100]$, indicative of ferromagnetic order. This is indeed consistent with the transition moving up in temperature [vertical arrows, Fig. 1(b)] with increasing applied field. At zero field the susceptibilities measured with $H_{ac} \parallel [100]$ and $H_{ac} \parallel [001]$ cross each other at a temperature just above T_C. This behavior is similar to that of the heavy fermion ferromagnet $YbNi_4P_2$ and of all other KL ferromagnets which order along the hard direction [9,32].

The temperature-dependent electrical resistivity in $YbIr_3Ge_7$ is typical of dense KL systems, as shown in Fig. 2. Metallic behavior with a positive resistivity coefficient ($d\rho/dT > 0$) is observed between 300 and 40 K. On further cooling, the resistivity shows a local minimum around 35 K, followed by a $-\ln T$ increase (dashed line) down to a coherence maximum around 6 K for $H = 0$ (red open symbols, Fig. 2), reflecting the incoherent Kondo scattering behavior. A drop in resistivity is seen as the temperature is further lowered through a magnetic phase transition
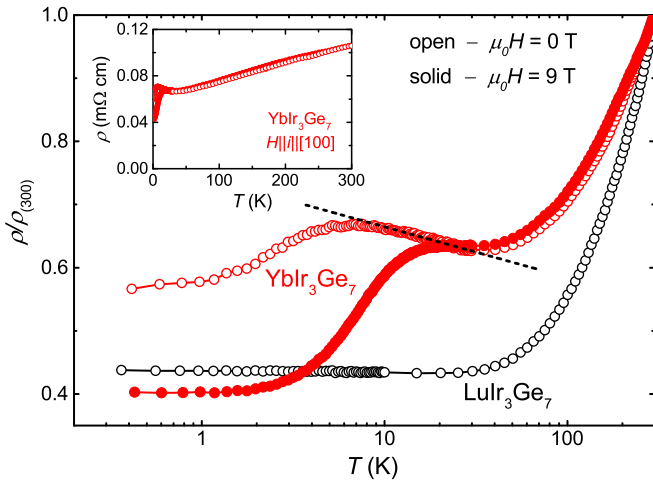
FIG. 2. Scaled temperature-dependent electrical resistivity ρ/ρ_{300} of $YbIr_3Ge_7$ (red circles) with $\mu_0 H = 0$ (open symbols) and 9 T (solid symbols) for $H || i || [100]$. The nonmagnetic polycrystalline analog $LuIr_3Ge_7$ is shown with black symbols. The dashed line in the main panel shows a $- \ln T$ increase in $\rho(T)$. The inset shows the absolute resistivity of $YbIr_3Ge_7$ with $\mu_0 H = 0$ and 9 T.

around 2.4 K, as shown more clearly in a derivative plot in Fig. S3 in the Supplemental Material. The resistivity in applied magnetic field $\mu_0 H = 9$ T (solid symbols, Fig. 2) shows the partial suppression of the Kondo effect and the FM fluctuations as the logarithmic increase disappears and the local maximum moves up in temperature.

A closer look at the ordered state with $T = 1.8$ K magnetization isotherms (Fig. 3) confirms the $H \parallel [100]$ ferromagnetic ordering (red solid circles), while the magnetization shows crossing around $\mu_0 H = 0.15$ T when $H \parallel [001]$ (blue, open symbols) and $H \parallel [100]$ (red, solid symbols): Small spontaneous magnetization (left inset) is observed for $H \parallel [100]$, while the $H \parallel [001]$ $M(H)$ is nearly linear at low
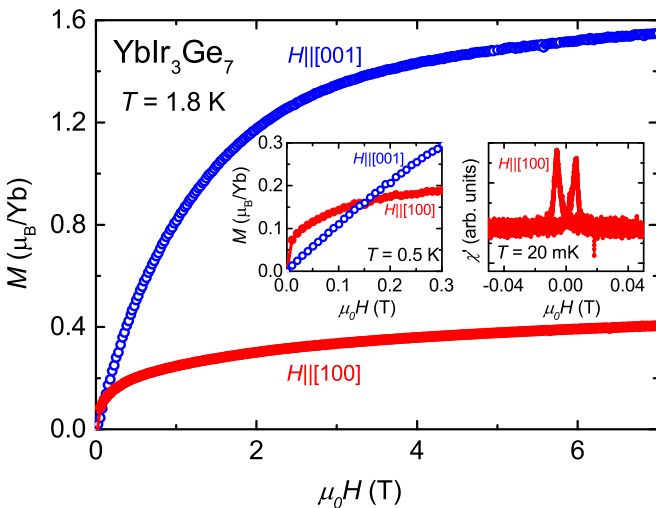

FIG. 3. Magnetization isotherm $M(H)$ at $T = 1.8$ K for $H \parallel [100]$ (solid red circles) and $H \parallel [001]$ (open blue circles). Left inset: Low field $M(H)$. Right inset: Ferromagnetic hysteresis in the ac susceptibility at 20 mK along $H \parallel [100]$.
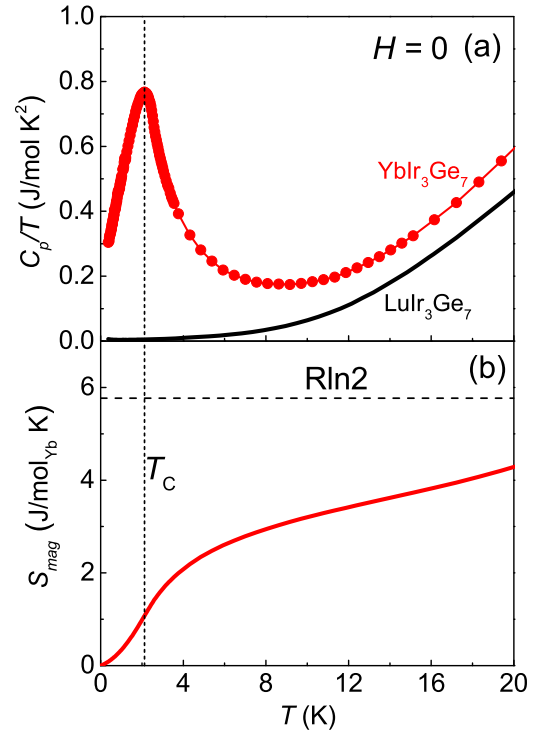

FIG. 4. (a) $H = 0$ specific heat of $YbIr_3Ge_7$ (red symbols and line) and $LuIr_3Ge_7$ (black line). (b) Magnetic entropy of $YbIr_3Ge_7$ with $S_{mag} = \int_0^T \frac{C_{mag}}{T} dT$, where $C_{mag} = C_p(YbIr_3Ge_7) - C_p(LuIr_3Ge_7)$.

H. A small magnetization hysteresis with a coercive field ≈ 6 mT is revealed at 20 mK in ac susceptibility measurements with $H \parallel [100]$, best illustrated in the $\chi'(H)$ plot (right inset). These features indicate that the FM ordering occurs with moments along the CEF hard direction [100]. The field along the CEF easy direction [001] rotates the moments to saturation without increasing much above 5 T, suggesting the absence of a relevant Van Vleck contribution [27]. The saturation magnetization of the ground-state Kramers doublet for $H \parallel$ [100] is reached at very small fields with $M_{[100]}^{sat} \approx 0.41 \mu_B$ whereas for $H \parallel [001]$ is reached at fields larger than 4 T with $M_{[001]}^{sat} \approx 1.55 \mu_B$. This yields a relatively large anisotropy factor of about 4. Therefore, assuming an anisotropic exchange interaction to explain the FM ordering with moments along the CEF hard axis [44] seems unlikely in the case of $YbIr_3Ge_7$, because this would necessitate an extremely large anisotropy for the exchange interaction [45].

Further evidence of the FM order in $YbIr_3Ge_7$ is shown by the specific heat (Fig. 4), marked by the peak at $T_C = 2.4$ K, consistent with the magnetization and resistivity derivatives (Fig. S2). As $T \rightarrow 0$, an enhanced electronic specific heat coefficient $\gamma_0 \sim \frac{C_p}{T} \approx 300$ mJ/mol K^2 is observed in $YbIr_3Ge_7$ (red), while the corresponding γ_0 for the nonmagnetic analog $LuIr_3Ge_7$ (black line) is, as expected, <5 mJ/mol K^2. We note that convergence between $YbIr_3Ge_7$ and the nonmagnetic analog does not occur up to 20 K. This is caused by an additional contribution to the specific heat of $YbIr_3Ge_7$ from population of the first excited crystal field level. Determination of the crystal electric field levels is left

to future inelastic neutron scattering experiments. The mass renormalization and the small magnetic entropy release at T_C, $S_{mag} \sim 17\%$ [Fig. 4(b)], suggest Kondo lattice formation in YbIr$_3$Ge$_7$, with a Kondo temperature $T_K \sim 14$ K estimated from $S_{mag}(0.5T_K) = 0.5R \ln 2$. This T_K estimate is in line with the temperature region where the resistivity exhibits Kondo resonance. YbIr$_3$Ge$_7$ thus appears to be a rare Yb-based KL ferromagnet with hard-axis moment ordering, and the first such compound crystallizing in a rhombohedral lattice.

In Ce- and Yb-based KLs, the development of FM order away from the CEF easy axis has been revealed in several compounds with different structures, and a wide range of T_C, from 0.15 K in YbNi$_4$P$_2$ [25] to 15 K in CeRuPO [22], while T_K ranges from 7 K in CeRuPO [22] up to 30 K in YbRhSb [15]. While YbIr$_3$Ge$_7$ has a three-dimensional crystal structure, YbNi$_4$P$_2$ has a quasi-one-dimensional crystal structure. This implies that the dimensionality of magnetic interactions and the relative magnitude of the magnetic and Kondo energy scales, i.e., the position in the Doniach phase diagram [1], have little to no effect on the FM order along the hard axis in these Kondo ferromagnets.

Krüger *et al.* [11] proposed a theoretical model to account for the hard-axis ferromagnetic order: They suggested that magnetic order along the hard axis can maximize the phase space for spin fluctuations in the easy plane, leading to a minimum in free energy. This is supported by the broadness of the specific heat peak (Fig. 4), hinting at the presence of critical fluctuations. In systems with a very strong easy-axis anisotropy, fluctuation-induced order might not appear and the transition would be mean field, as was observed in CeTiGe$_3$ (anisotropy factor of 10) [12]. Although YbIr$_3$Ge$_7$ shows a relatively high easy-axis anisotropy of a factor of 4, this is not strong enough to suppress fluctuations and the mechanism described by Krueger *et al.* might hold. Furthermore, a comparison of YbIr$_3$Ge$_7$ with the other isostructural Yb compounds is called for: YbIr$_3$Si$_7$ [37] and YbRh$_3$Si$_7$ [34] are both recently discovered highly anisotropic Kondo systems, with long-range magnetic order in the former, and an antiferromagnetic ground state in the latter as suggested by neutron scattering, with a small remanent magnetization of about 0.15μ_B/Yb along the [100] direction. Beyond the KLs showing hard-axis ordering, several other strongly correlated FMs [9] reveal that magnetic order away from the CEF easy axis is not an exception, but rather a frequent enough occurrence to warrant a thorough theoretical investigation. The "1-3-7" compounds (YbIr$_3$Ge$_7$ with ferromagnetic order and YbIr$_3$Si$_7$ long-range magnetic order [37], together with the antiferromagnet YbRh$_3$Si$_7$ [34]) have the Yb ions in the lowest point symmetry (trigonal) of all these KL compounds. With CEF effects inherently tied to the point symmetry of the magnetic moment, the observation of magnetic order away from the easy axis in different point symmetry cases underlines the difficulty of a generalized theory, which is left to a separate thorough theoretical study.

In conclusion, we report the discovery of a KL compound YbIr$_3$Ge$_7$ that shows FM ordering at $T_C = 2.4$ K, with the moment lying along the CEF hard direction. With a rhombohedral crystal lattice, this material expands this class of systems to include a different crystal structure. With relatively small T_C and T_K, YbIr$_3$Ge$_7$ is an ideal candidate to study FM QCP by chemical substitution, and to further develop existing theories to explain FM KL compounds.

[1] S. Doniach, Physica B&C (Amsterdam) **91**, 231 (1977).

[2] G. Stewart, Rev. Mod. Phys. **73**, 797 (2001).

[3] H. v. Löhneysen, A. Rosch, M. Vojta, and P. Wölfle, Rev. Mod. Phys. **79**, 1015 (2007).

[4] P. Gegenwart, T. Westerkamp, C. Krellner, Y. Tokiwa, S. Paschen, C. Geibel, F. Steglich, E. Abrahams, and Q. Si, Science **315**, 969 (2007).

[5] J. Paglione, T. Sayles, P.-C. Ho, J. Jeffries, and M. Maple, Nat. Phys. **3**, 703 (2007).

[6] B. Keimer and J. Moore, Nat. Phys. **13**, 1045 (2017).

[7] M. Brando, D. Belitz, F. M. Grosche, and T. R. Kirkpatrick, Rev. Mod. Phys. **88**, 025006 (2016).

[8] S. Ahamed, R. Moessner, and O. Erten, Phys. Rev. B **98**, 054420 (2018).

[9] D. Hafner, B. K. Rai, J. Banda, K. Kliemt, C. Krellner, J. Sichelschmidt, E. Morosan, C. Geibel, and M. Brando, arXiv:1901.04288.

[10] S. J. Yamamoto and Q. Si, Proc. Natl. Acad. Sci. USA **107**, 15704 (2010).

[11] F. Krüger, C. J. Pedder, and A. G. Green, Phys. Rev. Lett. **113**, 147001 (2014).

[12] V. Fritsch, O. Stockert, C.-L. Huang, N. Bagrets, W. Kittler, C. Taubenheim, B. Pilawa, S. Woitschach, Z. Huesges, S. Lucas *et al.*, Eur. Phys. J. Spec. Top. **224**, 997 (2015).

[13] P. Bonville, P. Bellot, J. Hodges, P. Imbert, G. Jéhanno, G. Le Bras, J. Hammann, L. Leylekian, G. Chevrier, P. Thuéry *et al.*, Physica B (Amsterdam) **182**, 105 (1992).

[14] K. Katoh, S. Nakagawa, G. Terui, and A. Ochiai, J. Phys. Soc. Jpn. **78**, 104721 (2009).

[15] Y. Muro, Y. Haizaki, M. S. Kim, K. Umeo, H. Tou, M. Sera, and T. Takabatake, Phys. Rev. B **69**, 020401(R) (2004).

[16] N. Tsujii, L. Keller, A. Dönni, and H. Kitazawa, J. Phys.: Condens. Matter **28**, 336002 (2016).

[17] K. Myers, S. Bud'ko, I. Fisher, Z. Islam, H. Kleinke, A. Lacerda, and P. Canfield, J. Magn. Magn. Mater. **205**, 27 (1999).

[18] G. André, F. Bourée, M. Kolenda, B. Leśniewska, A. Oleś, and A. Szytuła, Physica B (Amsterdam) **292**, 176 (2000).

[19] V. A. Sidorov, E. D. Bauer, N. A. Frederick, J. R. Jeffries, S. Nakatsuji, N. O. Moreno, J. D. Thompson, M. B. Maple, and Z. Fisk, Phys. Rev. B **67**, 224419 (2003).

[20] S. Araki, N. Metoki, A. Galatanu, E. Yamamoto, A. Thamizhavel, and Y. Ōnuki, Phys. Rev. B **68**, 024408 (2003).

[21] T. Takeuchi, A. Thamizhavel, T. Okubo, M. Yamada, N. Nakamura, T. Yamamoto, Y. Inada, K. Sugiyama, A. Galatanu, E. Yamamoto *et al.*, Phys. Rev. B **67**, 064403 (2003).

[22] C. Krellner and C. Geibel, J. Cryst. Growth **310**, 1875 (2008).

[23] C. Krellner, N. S. Kini, E. M. Brüning, K. Koch, H. Rosner, M. Nicklas, M. Baenitz, and C. Geibel, Phys. Rev. B **76**, 104418 (2007).

[24] C. Krellner, T. Förster, H. Jeevan, C. Geibel, and J. Sichelschmidt, Phys. Rev. Lett. **100**, 066401 (2008).

[25] C. Krellner, New J. Phys. **13**, 103014 (2011).

[26] C. Klingner, C. Krellner, M. Brando, C. Geibel, F. Steglich, D. Vyalikh, K. Kummer, S. Danzenbächer, S. Molodtsov, C. Laubschat *et al.*, Phys. Rev. B **83**, 144405 (2011).

[27] S. Lausberg, A. Hannaske, A. Steppke, L. Steinke, T. Gruner, L. Pedrero, C. Krellner, C. Klingner, M. Brando, C. Geibel *et al.*, Phys. Rev. Lett. **110**, 256402 (2013).

[28] T. Shimizu, H. Yasuoka, Z. Fisk, and J. L. Smith, J. Phys. Soc. Jpn. **56**, 4113 (1987).

[29] N. Tateiwa, T. D. Matsuda, Y. Haga, and Z. Fisk, Phys. Rev. B **89**, 035127 (2014).

[30] D. Belitz, T. R. Kirkpatrick, and T. Vojta, Phys. Rev. Lett. **82**, 4707 (1999).

[31] H. Kotegawa, T. Toyama, S. Kitagawa, H. Tou, R. Yamauchi, E. Matsuoka, and H. Sugawara, J. Phys. Soc. Jpn. **82**, 123711 (2013).

[32] A. Steppke, R. Küchler, S. Lausberg, E. Lengyel, L. Steinke, R. Borth, T. Lühmann, C. Krellner, M. Nicklas, C. Geibel *et al.*, Science **339**, 933 (2013).

[33] C. Krellner and C. Geibel, J. Phys.: Conf. Ser. **391**, 012032 (2012).

[34] B. K. Rai, S. Chikara, X. Ding, I. W. H. Oswald, R. Schönemann, V. Loganathan, A. M. Hallas, H. B. Cao, M. Stavinoha, T. Chen, H. Man, S. Carr, J. Singleton, V. Zapf, K. A. Benavides, J. Y. Chan, Q. R. Zhang, D. Rhodes, Y. C. Chiu, L. Balicas, A. A. Aczel, Q. Huang, J. W. Lynn, J. Gaudet, D. A. Sokolov, H. C. Walker, D. T. Adroja, P. Dai, A. H. Nevidomskyy, C.-L. Huang, and E. Morosan, Phys. Rev. X **8**, 041047 (2018).

[35] B. K. Rai, J. Banda, M. Stavinoha, R. Borth, D.-J. Jang, K. A. Benavides, D. Sokolov, J. Y. Chan, M. Nicklas, M. Brando *et al.*, Phys. Rev. B **98**, 195119 (2018).

[36] J. Banda, B. K. Rai, H. Rosner, E. Morosan, C. Geibel, and M. Brando, Phys. Rev. B **98**, 195120 (2018).

[37] M. Stavinoha, A. M. Hallas, W. A. Phelan, V. Loganathan, N. Caroca-Canales, C. Geibel, T. M. McQueen, A. H. Nevidomskyy, C.-L. Huang, and E. Morosan (unpublished).

[38] J. Remeika, G. Espinosa, A. Cooper, H. Barz, J. Rowell, D. McWhan, J. Vandenberg, D. Moncton, Z. Fisk, L. Woolf, H. Hamaker, M. Maple, G. Shirane, and W. Thomlinson, Solid State Commun. **34**, 923 (1980).

[39] B. K. Rai, I. W. Oswald, J. K. Wang, G. T. McCandless, J. Y. Chan, and E. Morosan, Chem. Mater. **27**, 2488 (2015).

[40] See Supplemental Material at http://link.aps.org/supplemental/10.1103/PhysRevB.99.121109 for results of single crystal and powder x-ray diffraction and refinements and other measurements.

[41] B. Chabot, N. Engel, and E. Parthé, Acta Crystallogr., Sect. B **37**, 671 (1981).

[42] P. Lorenz and W. Jung, Acta Crystallogr., Sect. E **62**, i173 (2006).

[43] G. Bowden, D. S. P. Bunbury, and M. McCausland, J. Phys. C **4**, 1840 (1971).

[44] E. C. Andrade, M. Brando, C. Geibel, and M. Vojta, Phys. Rev. B **90**, 075138 (2014).

[45] S. Hamann, J. Zhang, D. Jang, A. Hannaske, L. Steinke, S. Lausberg, L. Pedrero, C. Klingner, M. Baenitz, F. Steglich, C. Krellner, C. Geibel, and M. Brando, Phys. Rev. Lett. **122**, 077202 (2019).